

AD-A112 330

AD A-112 330

AD-E400 780

TECHNICAL REPORT ARLCD-TR-81044

**CARS SPECTROSCOPY OF GUN PROPELLANT FLAMES—  
HIGHER HOT BAND AND CONCENTRATION EFFECTS**

L. E. HARRIS

TECHNICAL  
LIBRARY

FEBRUARY 1982



**US ARMY ARMAMENT RESEARCH AND DEVELOPMENT COMMAND  
LARGE CALIBER  
WEAPON SYSTEMS LABORATORY  
DOVER, NEW JERSEY**

**APPROVED FOR PUBLIC RELEASE; DISTRIBUTION UNLIMITED.**

The views, opinions, and/or findings contained in this report are those of the author and should not be construed as an official Department of the Army position, policy or decision, unless so designated by other documentation.

Destroy this report when no longer needed. Do not return to the originator.

The citation in this report of the names of commercial firms or commercially available products or services does not constitute official endorsement or approval of such commercial firms, products, or services by the US Government.

UNCLASSIFIED

SECURITY CLASSIFICATION OF THIS PAGE (When Data Entered)

REPORT DOCUMENTATION PAGE		READ INSTRUCTIONS BEFORE COMPLETING FORM
1. REPORT NUMBER Technical Report ARLCD-TR-81044	2. GOVT ACCESSION NO.	3. RECIPIENT'S CATALOG NUMBER
4. TITLE (and Subtitle) CARS SPECTROSCOPY OF GUN PROPELLANT FLAMES-- HIGHER HOT BAND AND CONCENTRATION EFFECTS		5. TYPE OF REPORT & PERIOD COVERED
		6. PERFORMING ORG. REPORT NUMBER
7. AUTHOR(s) L. E. Harris		8. CONTRACT OR GRANT NUMBER(s)
9. PERFORMING ORGANIZATION NAME AND ADDRESS ARRADCOM, LCESL Applied Sciences Div (DRDAR-LCA-G) Dover, NJ 07801		10. PROGRAM ELEMENT, PROJECT, TASK AREA & WORK UNIT NUMBERS
11. CONTROLLING OFFICE NAME AND ADDRESS ARRADCOM, TSD STINFO Div, (DRDAR-TSS) Dover, NJ 07801		12. REPORT DATE February 1982
		13. NUMBER OF PAGES 38
14. MONITORING AGENCY NAME & ADDRESS (if different from Controlling Office)		15. SECURITY CLASS. (of this report) Unclassified
		15a. DECLASSIFICATION/DOWNGRADING SCHEDULE
16. DISTRIBUTION STATEMENT (of this Report) Approved for public release; distribution unlimited.		
17. DISTRIBUTION STATEMENT (of the abstract entered in Block 20, if different from Report)		
18. SUPPLEMENTARY NOTES		
19. KEY WORDS (Continue on reverse side if necessary and identify by block number)  Propellant                      Spectroscopy Combustion Flame CARS		
20. ABSTRACT (Continue on reverse side if necessary and identify by block number) Nitrogen Coherent Anti-Stokes Raman Scattering (CARS) spectra from nitrate-ester propellant flames contain several features not reported in nitrogen CARS spectra from other flames. Prominent among these features is a high intensity peak (30% maximum) 30 cm <sup>-1</sup> to the low energy side of the first hot band. Nitrogen CARS spectra from air/argon mixture containing from 1% to 30% air changed substantially with concentration but agreed with calculated spectra to better than 6%. Nitrogen CARS spectra from propane/air flames of (cont)		

DD FORM 1 JAN 73 1473

EDITION OF 1 NOV 65 IS OBSOLETE

UNCLASSIFIED

SECURITY CLASSIFICATION OF THIS PAGE (When Data Entered)

## 20. Abstract (cont)

various equivalence ratios showed a resolved second hot band, Q(32) at 2,269  $\text{cm}^{-1}$  and the presence of the third hot band, Q(43), near 2,241  $\text{cm}^{-1}$ . Temperatures determined from Q(32) agreed, within experimental error, with those determined with Q(10) at 2,296  $\text{cm}^{-1}$ . Temperature trends for the various equivalence ratios agreed with thermochemical predictions, allowing the accuracy to be assessed at better than 5%. The good agreement of nonplanar and planar BOXCARS validated the earlier planar BOXCARS measurements. Nitrogen CARS calculations agreed well with experimental propellant spectra at the 10% nitrogen concentration expected from thermochemical calculations. The calculated spectra show the presence of Q(32) near 30% maximum intensity as seen in the propellant spectra.

## CONTENTS

	Page
Introduction	1
Experimental	2
Results	2
Discussion	4
Conclusions	5
References	7
Distribution List	25

## TABLES

	Page
1 Concentration of air (%) in air/ar mixtures at 300 K	9
2 Thermochemical calculations	10
3 Temperature determined from nonplanar BOXCARS	10
4 Comparison of experimental and theoretical temperatures	11
5 Comparison of planar and nonplanar BOXCARS temperatures	11

## FIGURES

1 Phase matching	13
2 CARS spectrometer	14
3 Normalized nitrogen CARS spectra from room temperature air/argon mixture containing 0% to 23% air	15
4 Normalized nitrogen CARS spectra from room temperature air/argon mixture containing 3% to 100% air	16
5 Experimental (.) and calculated N <sub>2</sub> CARS spectra at room temperature in a 9% air/argon mixture (nonplanar CARS)	17
6 Experimental (.) and calculated N <sub>2</sub> CARS spectra at room temperature in a 20% air/argon mixture (nonplanar CARS)	18
7 Experimental (.) and theoretical $\log [(I_{10} - I_{NR})/I_{NR}]$ where $I_{10}$ and $I_{NR}$ are the maximum intensities of nitrogen Q <sub>10</sub> and the nonresonant susceptibility versus $\log [C(\%)]$	19
8 Experimental (.) and calculated N <sub>2</sub> CARS spectra of room temperature air (nonplanar CARS)	20
9 Calculated N <sub>2</sub> CARS spectra with temperature varying from 1,500 - 3,000 K at 250 K intervals	20
10 Calculated N <sub>2</sub> CARS spectra with temperature varying from 1,900 - 2,000 K at 20 K intervals	21
11 Experimental (.) and calculated N <sub>2</sub> CARS spectra for 1.02 equivalence ratio propane/air flame at T = 2,000 K (nonplanar CARS)	21
12 Experimental (.) and calculated N <sub>2</sub> CARS spectra for 0.81 equivalence ratio propane/air flame at T = 1,930 K (nonplanar CARS)	22

- 13 Experimental (.) and calculated  $N_2$  CARS spectra for 1.02 equivalence ratio propane/air flame at  $T = 2,020$  K (planar CARS) 22
- 14 Calculated  $N_2$  CARS spectra at 2,500 K for flame products with 25, 50, 70, and 100% of the stoichiometric percentage of air 23

## INTRODUCTION

Measurements of temperature and concentration spatial profiles in propellant and related laboratory flames should provide experimental results needed to identify the controlling mechanisms of propellant combustion. These measurements are difficult to make with conventional methods since propellant flames are often transient, incandescent, and particle-laden. Coherent Anti-Stokes Raman Scattering (CARS), due to its high intensity and coherent nature, provides a means of probing propellant flames. The CARS signal can be generated from a spatially, well defined region in the flame on the order of  $1 \text{ mm}^3$  within the time duration of the laser pulse. CARS involves the interaction of two high intensity laser beams, the pump and Stokes beams, at angular frequencies  $\omega_p$  and  $\omega_s$ , respectively. When  $\omega_p$  and  $\omega_s$  are separated by a Raman resonance frequency, CARS,  $\omega_{as}$  is generated at the anti-Stokes frequency. CARS signal strength is proportional to the square of the modulus of the third-order electric susceptibility,  $|\chi^{(3)}|^2$ . The susceptibility is the sum of a resonant,  $\chi_r$ , and nonresonant term,  $\chi_{nr}$ .  $\chi_r$  can be expanded into a real and imaginary term.

$$|\chi^{(3)}|^2 = |\chi_r' + i\chi_r'' + \chi_{nr}|^2 \quad (1)$$

$\chi_r'$  and  $\chi_r''$  have dispersive and resonant line shapes, respectively; therefore, at low concentration the CARS lineshape becomes dispersive.

$$|\chi^{(3)}|^2 = |\chi_r' \chi_{nr} + \chi_{nr}^2| \quad (2)$$

Nitrogen CARS spectra have been reported for nitrate-ester propellant flames (ref 1 through 3). The propellant spectra contained several features that had not been reported in nitrogen CARS spectra from other flames. The novel features in the propellant nitrogen CARS spectra can be attributed to the lower concentration of nitrogen, the high temperature of the flame, and the lower resolution necessitated by the low intensity of the spectra. Prominent among the novel features was a high intensity (30% maximum) peak  $30 \text{ cm}^{-1}$  to the low energy side of the first hot band. This peak had not been reported in previous investigations on flames. To determine the nature of the novel spectral features, the following investigations were undertaken:

1. Nitrogen CARS spectra from air/argon mixtures with nitrogen at concentrations near that in the propellant flame (10%).

2. Nitrogen CARS spectra from propane/air flames of various equivalence ratios with emphasis on the behavior of the second hot band. Thermochemical calculations were performed to assess the accuracy of the experimentally determined temperatures.

## EXPERIMENTAL

CARS spectra were generated using apparatus with both planar and nonplanar BOXCARS (ref 4) phasematching (fig. 1), using the apparatus shown in figure 2. The pump laser beam,  $\omega_l$  is produced by a Quanta-Ray DCR-1A Nd/YAG laser. The output of the Nd/YAG laser at 1.06 microns (700 mj) is doubled to generate the pump beam,  $\omega_l$ , at 5,320 Å (250 mj) with a bandwidth of about  $1 \text{ cm}^{-1}$ . The pump beam is separated from the primary beam using prisms. Forty percent of the pump beam is split off ( $BS_1$ ) to pump a dye laser to generate the Stokes beam,  $\omega_s$ . The dye laser is operated broadband to produce 30 mj centered at 6,070 Å with a bandwidth of about  $150 \text{ cm}^{-1}$ . To achieve BOXCARS geometry, the pump is split using a 50% beamsplitter,  $BS_2$ . In planar BOXCARS, the  $\omega_l$  beam is reflected from a dichroic (DC) which transmits the stokes beam, and  $\omega_l'$  is separately reflected along another path so that the pump beams are separated at the focusing lens. The planar BOXCARS signal,  $\omega_{as}$ , which is generated along  $\omega_l$ , is isolated by prism and spatial filtering. In nonplanar BOXCARS,  $\omega_s$  is introduced below the plane of  $\omega_l$  at the focusing lens to produce a spatially isolated  $\omega_{as}$  which is focused onto the slits of a monochromator fitted with a PAR SIT detector. The signal from the detector is sent to an OMA2 for processing.

In these experiments a 200-mm focusing lens was used with a pump beam crossing angle of  $5^\circ$  in planar BOXCARS. In nonplanar BOXCARS, the  $\omega_l$ ,  $\omega_l'$ , and  $\omega_s$  beams are situated on a circle of 1-inch radius at the focusing lens with  $\omega_l$  and  $\omega_l'$  in the horizontal plane and  $\omega_s$  in the vertical plane. A 1/4-meter monochromator equipped with a 1,800 line/mm grating and 100-micron slits was used for dispersal of  $\omega_{as}$ . Neon spectral lines were used to determine the resolution and wavelength calibration of the monochromator.

## RESULTS

Temperature is determined by comparison of the experimental  $N_2$  spectra with spectra calculated according to the procedure given by Hall (ref 5) using parameters given in references 5 through 7. The spectral parameters of  $\omega_s$  were determined by flowing argon with some admixture of air through the burner to generate nonresonant CARS spectra which mirrors the spectral shape of  $\omega_s$ . This spectra, in addition to providing the spectral parameters of  $\omega_s$  illustrates the dependence of CARS spectra on concentration. CARS spectra from room temperature air/argon mixtures containing from 1% to 100% air are shown in figures 3 and 4. A comparison of calculated and experimental spectra in a 9% and 20% air/argon mixture is shown in figures 5 and 6, respectively. The ratio of the maximum intensities at  $Q_{10}$  and the nonresonant susceptibility is a direct measure of the concentration. Experimental and calculated maximum  $Q_{10}$  to nonresonant susceptibility ratio are given in table 1 and shown in figure 7. The agreement between theory and experimental is given in table 1 as 6.1%. The depth of the dip goes to increasingly larger intensity as the concentration decreases. A similar effect of concentration on CARS CO spectra was observed by Eckbreth (ref 4). The spectrum shown in figure 8 was determined using nonplanar BOXCARS with a slit width of  $6.4 \text{ cm}^{-1}$  and  $2.38 \text{ cm}^{-1}$  per channel as determined from the room temperature  $N_2$  CARS spectrum shown in figures 5, 6, and 7. The spectral parameters determined for  $\omega_s$  from

spectra similar to that in figure 5 were  $\omega_s^{\max}$  at  $16,500 \text{ cm}^{-1}$  with full width at half height (FWHH) of  $130 \text{ cm}^{-1}$ . These experimental parameters pertain to all the other reported nonplanar BOXCARS spectra. The experimentally determined parameters were used to generate CARS spectra with temperatures varying from 1,500 to 3,000 K (at 250-K intervals) which are shown in figure 9. The  $Q_{10}$ ,  $Q_{21}$ , and  $Q_{32}$  peaks are seen to be clearly resolved at near to 2,325, 2,296, and 2,269  $\text{cm}^{-1}$ , respectively. The bands shift slightly to the red as the temperature is raised. A shoulder near 2,241  $\text{cm}^{-1}$ , attributable to  $Q_{43}$ , is seen to be almost resolved at 3,000 K. The average calculated separation between peaks is  $28 \text{ cm}^{-1}$ . The relative height of the  $Q_{10}$  peak determined experimentally was previously used to determine temperature from the calculated spectra (ref 4). Calculations made at small intervals (20 K) such as shown in figure 10 are, in practice, used to determine temperature.

Measurements of  $\text{N}_2$  CARS spectra were made immediately above the reaction zone on the centerline of the burner with both nonplanar and planar BOXCARS. The nonplanar results were obtained at fuel/air equivalence ratios of 1.02, 0.81, and 1.27. The 1.02 and 0.81 equivalence ratio results are shown in figures 11 and 12, respectively, along with the calculated spectra. (The 1.27 equivalence ratio results look very similar to the 0.81 results.) The planar results are given in figure 13.

The  $Q_{32}$  peak is resolved and occurs at the calculated frequency. The  $Q_{43}$  is not clearly resolved but can be identified as occurring at the calculated position.

The results of the thermochemical calculations performed with the NASA-LEWIS computer code at the experimental equivalence ratios are given in table 2. The temperatures determined from the  $Q_{21}$  and  $Q_{32}$  peaks,  $T_{21}$  and  $T_{32}$ , respectively, are given in table 3. The temperatures determined from two different spectra for the equivalence ratio 1.02 showed that the precision of the method was quite good. The agreement between  $T_{21}$  and  $T_{32}$  was within the accuracy of the experimental data; however,  $T_{32}$  was systematically lower than  $T_{21}$ . This may result from slight inaccuracies in the  $\omega_s$  parameters. Since  $T_{21}$  and  $T_{32}$  agreed within the accuracy of the data, no attempt was made to vary the  $\omega_s$  parameters. A comparison of the experimental and thermochemically calculated temperatures is given in table 4. The experimentally determined temperatures are lower than the calculated adiabatic flame temperatures by about 10% on average. This is attributable to heat loss by radiation, thermal conduction, or diffusion which vary with burner design. The magnitude of the error is consistent with previous studies (ref 8). The error determined from the normalized temperatures (assuming constant percentage heat loss) is consistent with the known errors in CARS temperature determination and the flowmeters. The error is predominately in the flowmeters since the precision of CARS was shown above to be better.

Temperatures were also determined at the equivalence ratio of 1.02 with the planar BOXCARS configuration. The  $\omega_s$  parameters were  $\omega_s^{\max}$  at  $16,497 \text{ cm}^{-1}$  with a width of  $153 \text{ cm}^{-1}$ . The slit width determined from the room temperature spectra was  $9.6 \text{ cm}^{-1}$  with  $2.336 \text{ cm}^{-1}$  per channel. A comparison of the planar and nonplanar  $T_{21}$  and  $T_{32}$  temperatures is shown in table 5. The agreement is very good considering the substantial changes made in the apparatus.

## DISCUSSION

The high temperature and low concentration (less than 30%) of each product in propellant flames introduce features of  $N_2$  CARS not previously reported. In addition, to attain the required intensity, lower resolution than that used in other studies was used.

Concentration as shown in figures 3, 4, 5, and 6 alters the appearance of  $N_2$  CARS spectra at room temperature. The effect of concentration at 2,500 K is shown in figure 14. At higher concentration of room temperature spectra, the calculated maximum intensity falls as the square of the concentration. However, at high temperatures the steepness of the decline of the signal with concentration begins to moderate at 50% air as opposed to room temperature where moderation does not begin to occur until 5% air is reached. This difference occurs because the high temperature spectra is spectrally wider than the room temperature spectra. As a consequence, the maximum intensity at high temperature is less relative to the nonresonant susceptibility than at low temperatures. At the 10% level, the signal is decreased from the 100% level by factors of 85 and 25 at 298 and 2,500 K, respectively. This lessening of the square root dependence of intensity on concentration makes possible CARS measurements in flames at lower levels of the concentration of products.

The  $Q_{32}$  hot band is much more sensitive to concentration than  $Q_{21}$ . At the 50% level,  $Q_{32}$  has more than doubled in intensity while  $Q_{21}$  has only increased by a few percent. Thus, high temperature and low concentration result in high intensity of  $Q_{32}$  in the previously reported propellant spectra. The results given in tables 3 through 5 establish the utility of  $Q_{32}$  for measurement of temperature. The results in figure 14 indicate that  $Q_{32}$  is useful for estimation of the concentration in the range 10% to 100%, given an approximate temperature from  $Q_{10}$ . Below 10%, if a spectrum can be obtained, the depth of the dip on the high energy side of  $Q_{10}$  is useful for estimation of the concentration. These initial estimates of temperature and concentration should be used as input to a least-squares routine to accurately determine temperature and concentration from the spectrum. In the situation where all species are present below the 30% level, it becomes necessary to determine temperature and concentration simultaneously.

The results obtained in comparison of planar and nonplanar BOXCARS indicate that configuration can have an effect on the resolution of the observed spectra. Nonplanar and planar BOXCARS were observed to give spectral resolutions of 6.4 and 9.6  $cm^{-1}$ , respectively. This may be due to some distortion of the spectrum resulting from the additional optical elements in planar BOXCARS. It is also possible that the positioning of the CARS signal was not optimized in the planar BOXCARS configuration. The intensity of the CARS signal was higher in the planar configuration which may have some effect on the resolution. Since the spectra and temperatures were the same for planar and nonplanar BOXCARS, no clipping by the slit of the prism-dispersed planar BOXCARS signal is evident. However, the  $cm^{-1}/channel$  of the planar BOXCARS signal was reduced from the 2.34 to 2.20 to adequately match the spectrum. This was not necessary in nonplanar BOXCARS and may reflect the additional dispersion due to the prism used in planar BOXCARS.

The spectral features observed in propane/air flames and air/air mixtures can be used to interpret the previously reported propellant spectra which are intermediate between the 25% air (18% N<sub>2</sub>) and 50% air (35% N<sub>2</sub>) spectra shown in figure 14. The calculated concentration of N<sub>2</sub> in the propellant was 10%. However, the nonresonant susceptibility in the propellant flame is higher than the value used for the propane/air flame; this would reduce the computed concentration. Differences in spectral properties of  $\omega_s$  may account for the remaining difference. Alternately there could be some initial mixing in of air. Further work will be needed to resolve this. This spectral resolution of 8 cm<sup>-1</sup> is consistent with the use of planar BOXCARS to obtain the propellant spectra.

The previously obtained propellant spectrum is in satisfactory agreement with calculations, properly accounting for concentration and using the Q<sub>32</sub> hot band. Further measurements of M31 and similar propellants are planned. These propellants would have a flame temperature near 2,500 K and N<sub>2</sub> concentration near 30%. The 10<sup>2</sup>-10<sup>3</sup> counts per shot obtained in the 2,000 K propane/air flame would be reduced by a factor of 2.5 by an increase of temperature to 2,500 K and a factor of 4 by a decrease of N<sub>2</sub> concentration to 30% to give an overall order of magnitude reduction in signal which would still be adequate for making measurements. CH<sub>4</sub>/N<sub>2</sub>O and other similar flames will be studied to aid in interpretation of the propellant flames.

#### CONCLUSIONS

Nitrogen CARS spectra from air/air mixtures with N<sub>2</sub> present at concentrations from 1% to 100% air changed substantially with concentration but agreed well with calculated spectra. Nitrogen CARS spectra from propane/air flames of various equivalence ratios showed a resolved second hot band, Q<sub>32</sub>, and the presence of the third hot band, Q<sub>43</sub>. Temperatures determined from Q<sub>32</sub> were in accord, within experimental error, with those determined from the first hot band, Q<sub>21</sub>. Temperature trends for the various equivalence ratios agreed with the predictions of NASA-LEWIS thermochemical-calculations. The correlation with thermochemical-chemical calculations allowed the accuracy of the experimental measurements to be assessed at better than 5%. Nonplanar BOXCARS gave spectra similar, within experimental error, to that obtained using planar BOXCARS, thus verifying previous work employing planar BOXCARS. Calculations at near the temperature of propellant flames are similar to propellant flame spectra previously obtained at the 10% concentration expected from thermochemical calculations. The calculated spectra show the presence of Q<sub>32</sub> near 30% maximum intensity as seen in the experimental propellant spectra.

## REFERENCES

1. L. E. Harris and M. McIlwain, "CARS Spectroscopy of Gun Propellant Flames," Fast Reactions in Energetic Systems, ed. C. Capellos and R. F. Walker, Reidel, 1981, pp 473-484.
2. M. McIlwain and L. E. Harris, 17th JANNAF Combustion Meeting, vol II, CPIA Publication 329, 1980, pp 379-389.
3. L. E. Harris and M. McIlwain, "CARS Spectroscopy of Gun Propellant Flames," Technical Report ARLCD-TR-81007, ARRADCOM, Dover, NJ, September 1981.
4. A. C. Eckbreth and R. J. Hall, Combust. Science and Technology, vol 25, 1981, p 175.
5. R. J. Hall, Combust. Flame, vol 35, 1979, p 47.
6. R. J. Hall, Applied Spectroscopy, vol 34, 1980, p 100.
7. A. Owyong and L. A. Rahn, IEEE, J. Quant. Elect., QE-15, 1979, pp 25D-26D.
8. A. G. Gaydon and H. G. Wolfhard, Flames, fourth edition, Chapman and Hall, London, 1979, p 324.

Table 1. Concentration of air (%) in air/ar mixtures at 300 K

<u>*C<sub>experimental</sub></u> <u>(%)</u>	<u>*C<sub>calculated</sub></u> <u>(%)</u>	<u>Difference</u> <u>between columns</u> <u>1 and 2</u>	<u>% Difference</u> <u>between columns</u> <u>1 and 2</u>
7.06	5.92	1.1	16.1
8.54	7.80	0.7	8.7
12.0	11.6	0.4	3.3
13.8	14.8	-1.0	7.2
19.7	18.8	0.9	4.5
22.8	22.7	0.1	0.50
30.2	31.0	<u>-0.8</u>	<u>2.65</u>
Mean ( $\sigma$ )		0.7 (0.3)	6.1 (5.1)

---

\* Concentration

Table 2. Thermochemical calculations

<u>Equivalence ratio</u>	<u>Temperature (K)</u>	<u>N<sub>2</sub> (%)</u>	<u>H<sub>2</sub>O (%)</u>	<u>CO<sub>2</sub> (%)</u>	<u>CO (%)</u>	<u>H<sub>2</sub> (%)</u>
0.81	2,085	73	13	10	1	-
1.01	2,273	71	15	10	2	-
1.27	2,143	67	15	7	7	3

Table 3. Temperature determined from nonplanar BOXCARS

<u>Equivalence ratio</u>	<u>Temperature (K)</u>					
	<u>T<sub>21</sub></u>	<u>(σ)*</u>	<u>T<sub>32</sub></u>	<u>(σ)</u>	<u>T<sub>avg</sub></u>	<u>(σ)</u>
0.81	1,932	(29)	1,843	(69)	1,888	(63)
1.02	2,003	(54)	1,934	(116)	1,969	(49)
1.02	1,990	(38)	1,913	(74)	1,952	(54)
1.27	1,914	(29)	1,853	(81)	1,884	(43)

Table 4. Comparison of experimental and theoretical temperatures

Equivalence ratio	Temperature (K)					
	$T_{calc}$	$T_{21}^a$	$\Delta T$	$T_{calc}^b$	$T_{21}^b$	$\% \Delta T$
1.02	2,276	1,997	279	1	1	
1.27	2,143	1,914	229	0.94	0.96	2
0.81	2,085	1,932	153	0.92	0.97	5

<sup>a</sup>  $\Delta T = T_{cal} - T_{21}$ .

<sup>b</sup> Normalized temperature.

Table 5. Comparison of planar and nonplanar BOXCARS temperatures

Configuration	Temperature (K)					
	$T_{21}$	( $\sigma$ )	$T_{32}$	( $\sigma$ )	$T_{avg}$	( $\sigma$ )
Planar	2,021	(48)	1,902	(109)	1,962	(84)
Nonplanar	1,990	(38)	1,913	(74)	1,952	(54)

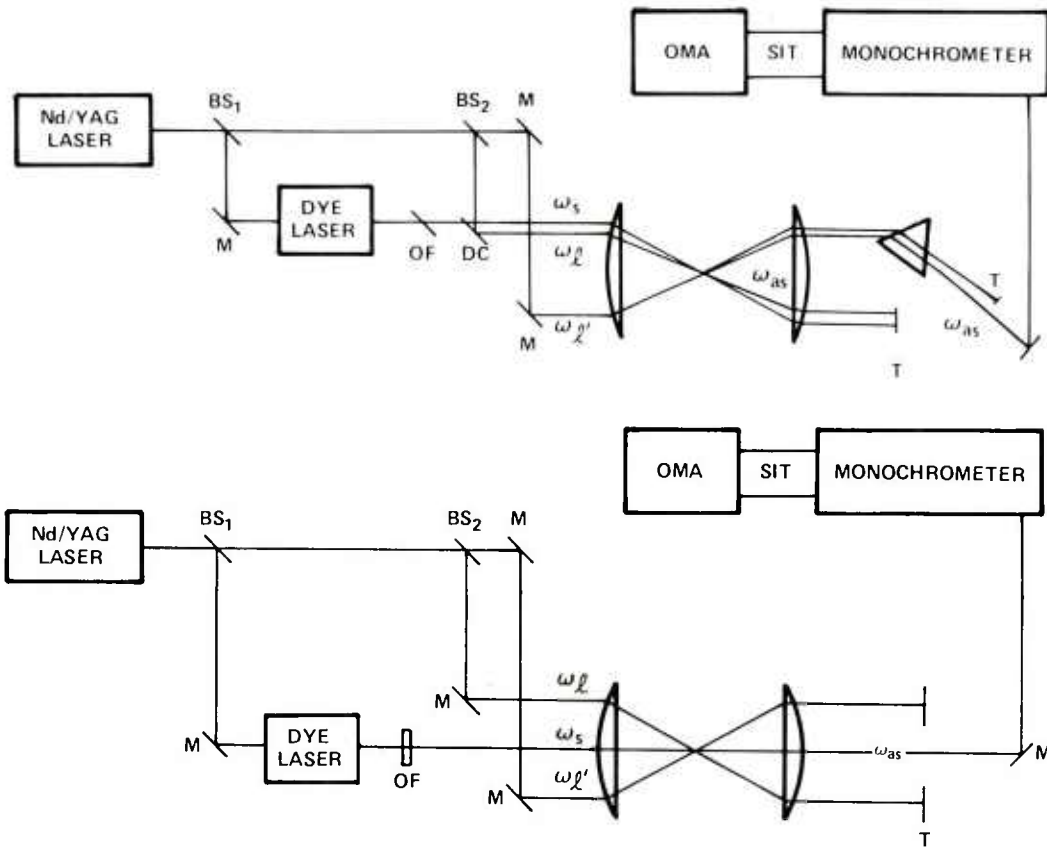
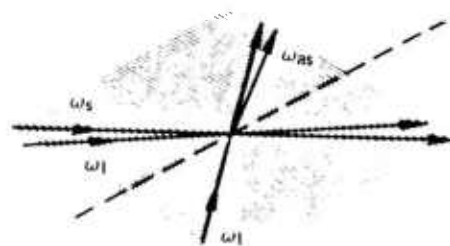
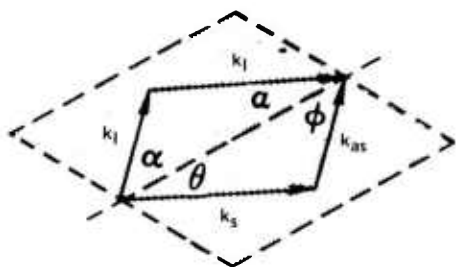


Figure 1. Phase matching

a) Planar

BOXCARS



b) Folded

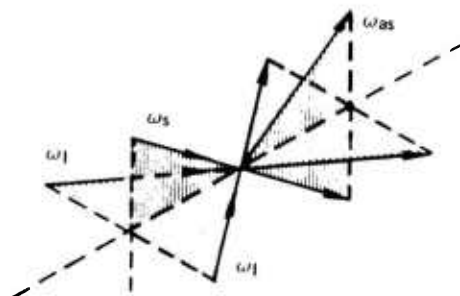
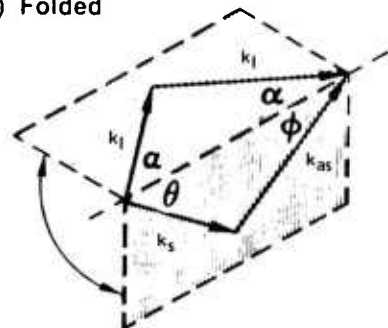


Figure 2. CARS spectrometer

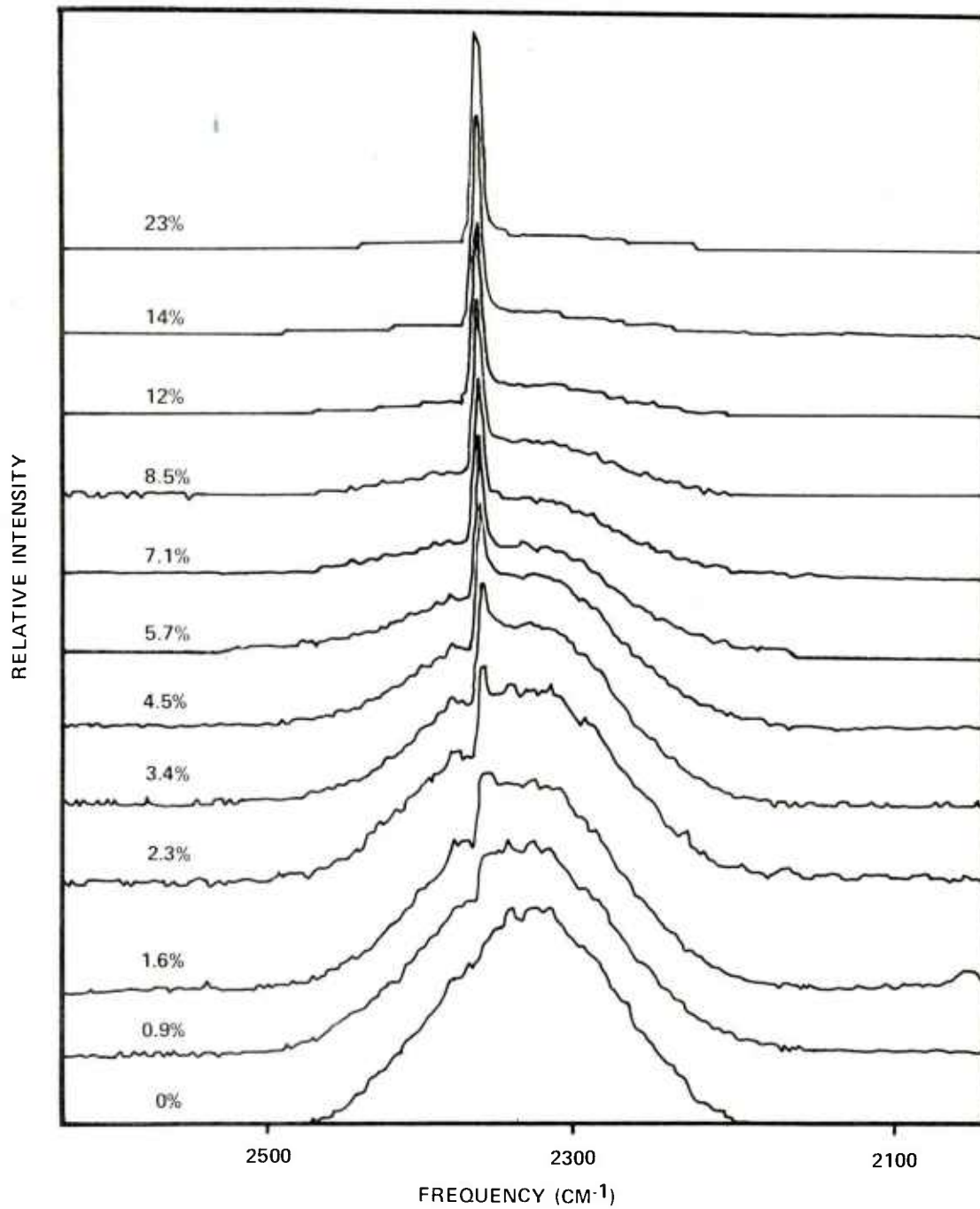


Figure 3. Normalized nitrogen CARS spectra from room temperature air/argon mixture containing 0% to 23% air

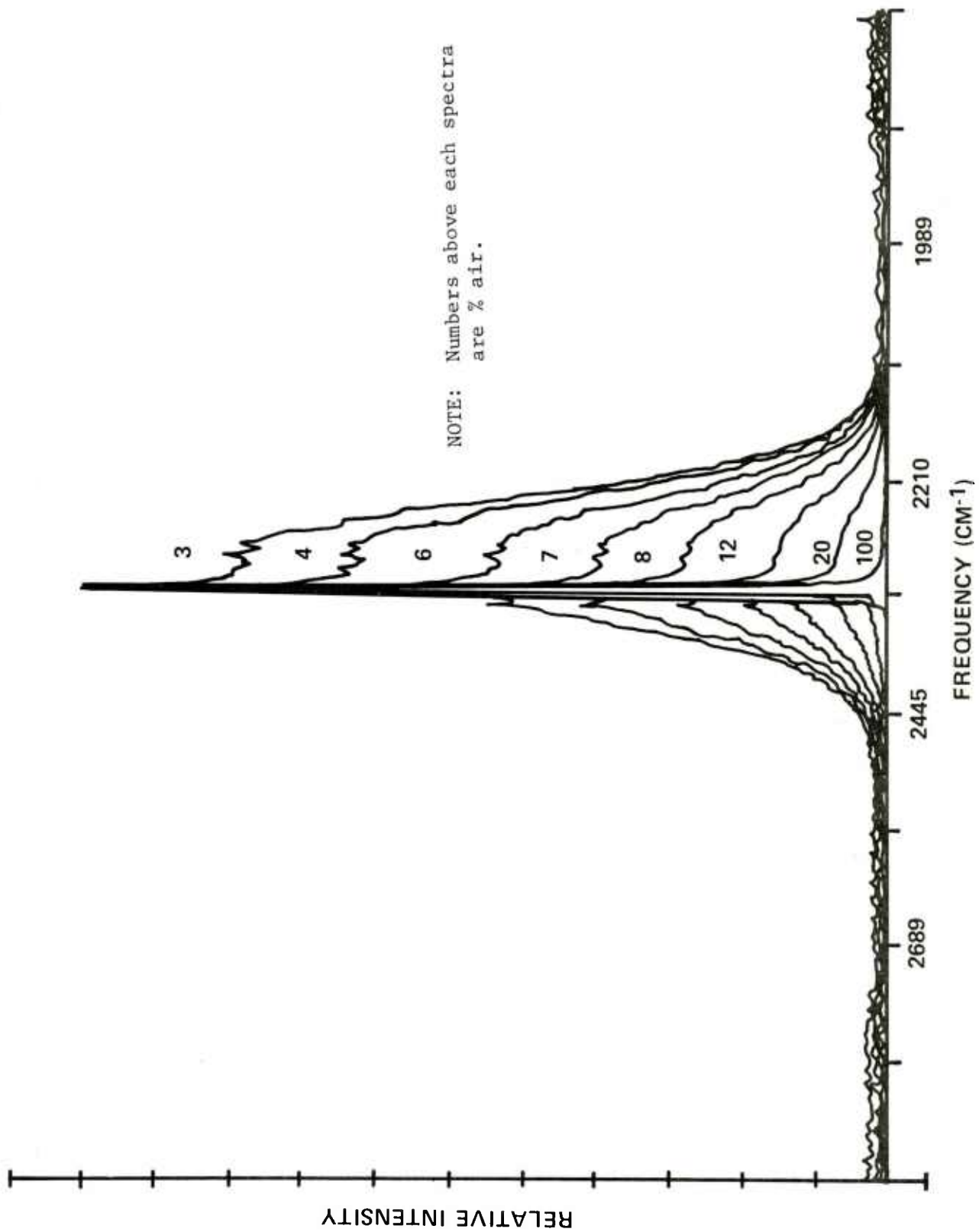


Figure 4. Normalized nitrogen CARS spectra from room temperature air/argon mixtures containing 3% to 100% air

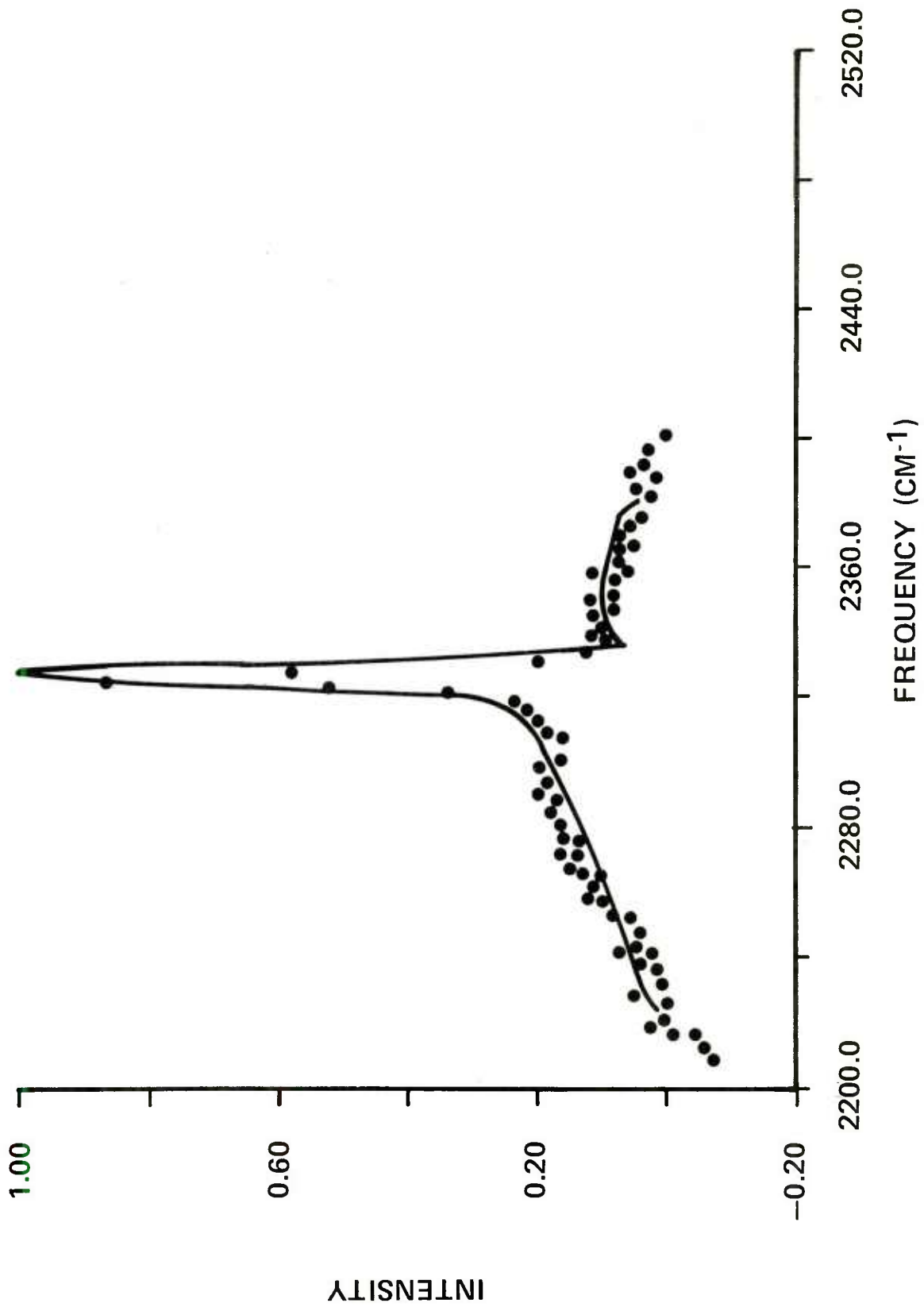


Figure 5. Experimental (•) and calculated N<sub>2</sub> CARS spectra at room temperature in a 9% air/argon mixture (nonplanar CARS)

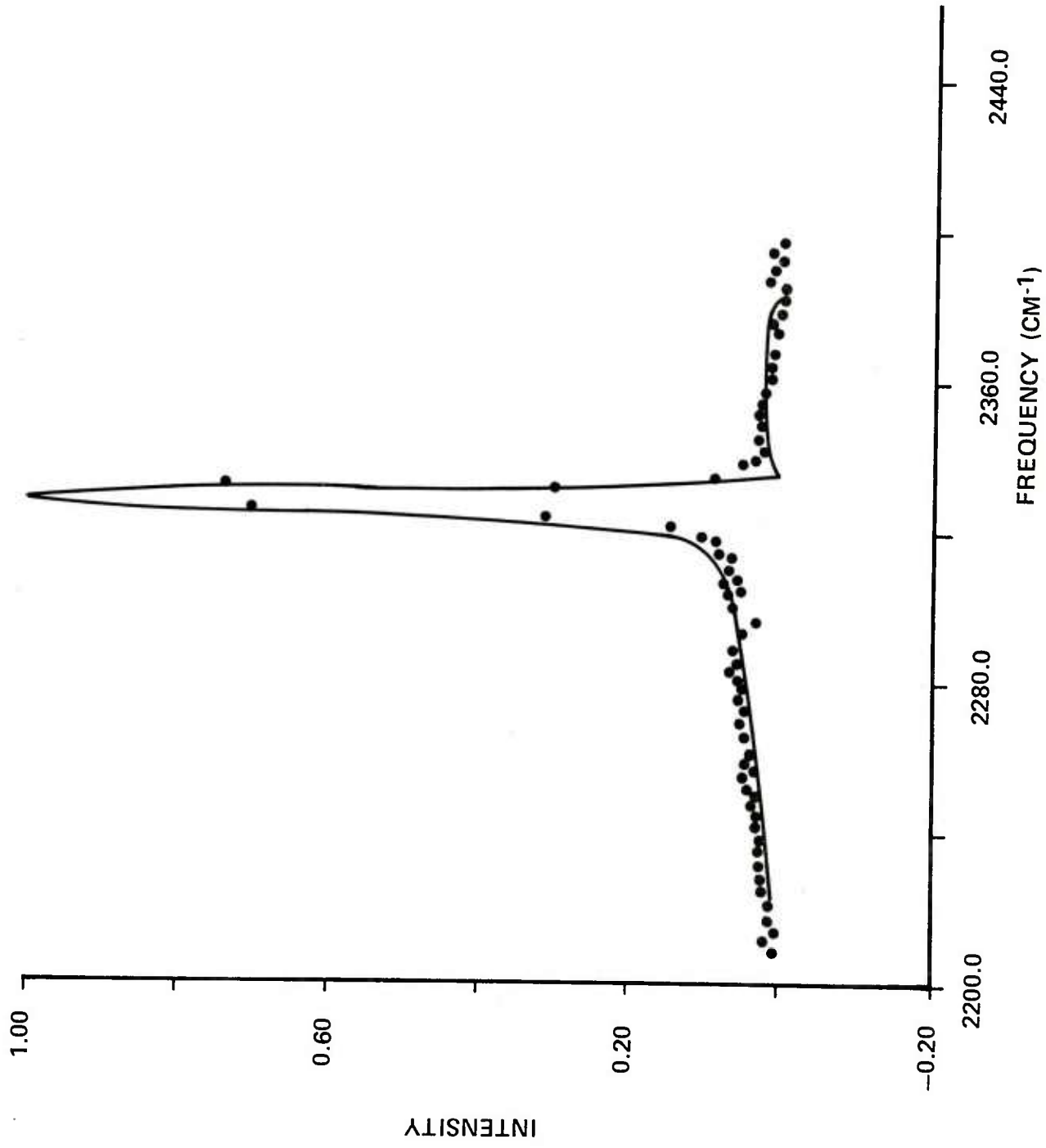


Figure 6. Experimental (.) and calculated N<sub>2</sub> CARS spectra at room temperature in a 20% air/argon mixture (nonplanar CARS)

## AIR/AR MIXTURES AT 300K

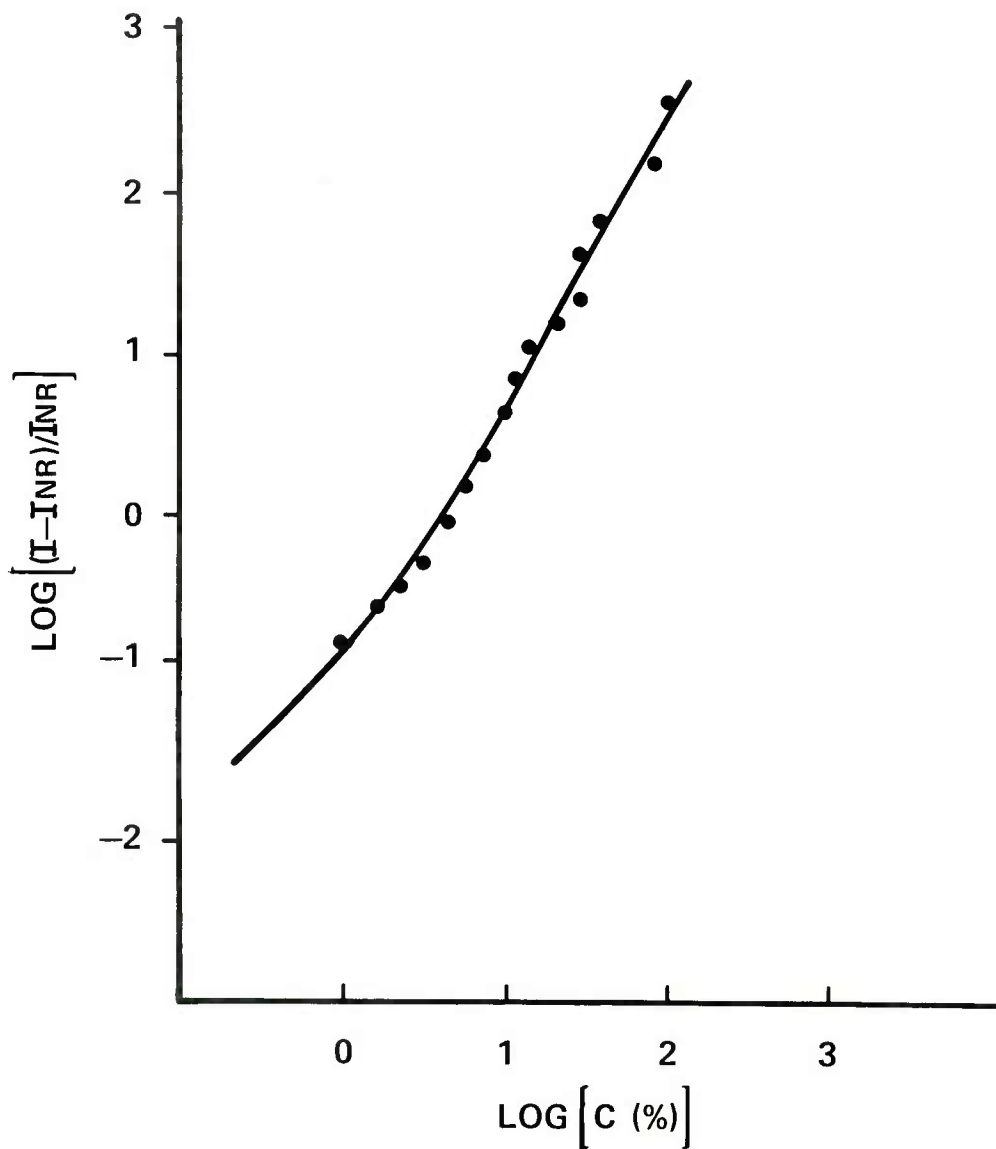


Figure 7. Experimental (.) and theoretical  $\log [(I_{10} - I_{NR}) / I_{NR}]$  where  $I_{10}$  and  $I_{NR}$  are the maximum intensities of nitrogen  $Q_{10}$  and the nonresonant susceptibility versus  $\log [C(\%)]$

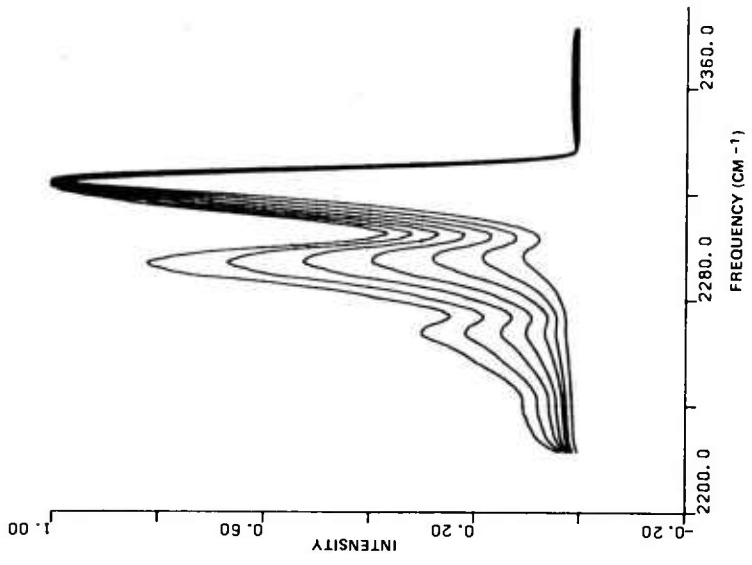


Figure 9. Calculated N<sub>2</sub> CARS spectra with temperature varying from 1,500 - 3,000 K at 250 K intervals

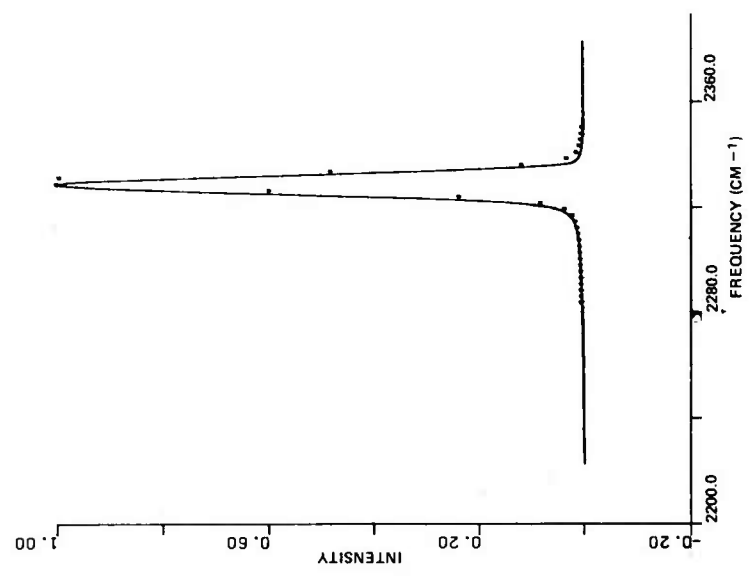


Figure 8. Experimental (•) and calculated N<sub>2</sub> CARS spectra of room temperature air (nonplanar CARS)

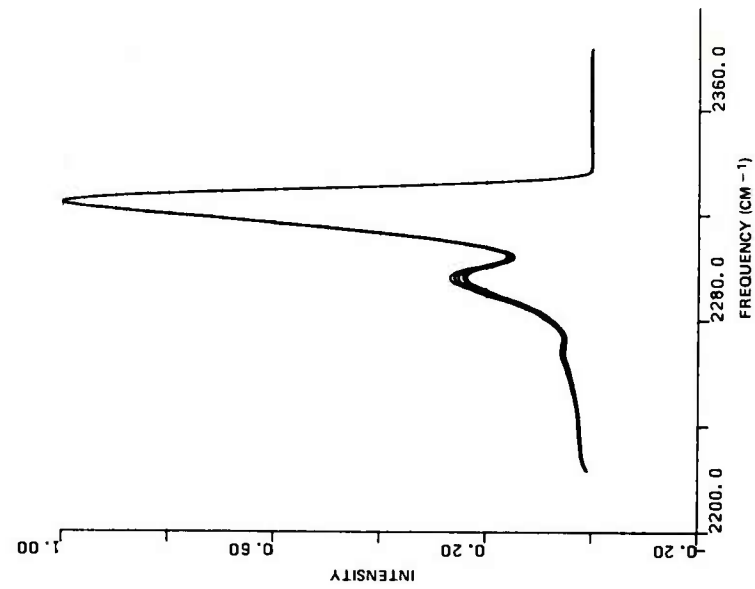


Figure 10. Calculated  $N_2$  CARS spectra with temperature varying from 1,900 - 2,000 K at 20 K intervals

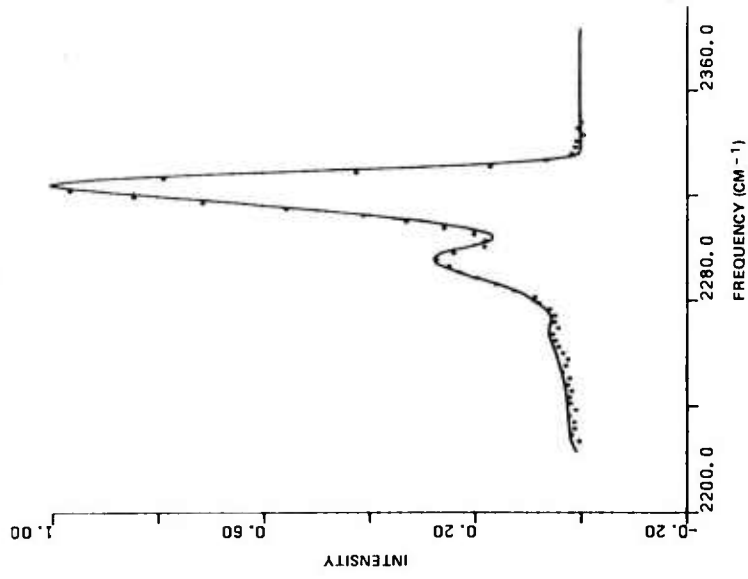


Figure 11. Experimental (.) and calculated  $N_2$  CARS spectra for 1.02 equivalence ratio propane/air flame at  $T = 2,000$  K (nonplanar CARS)

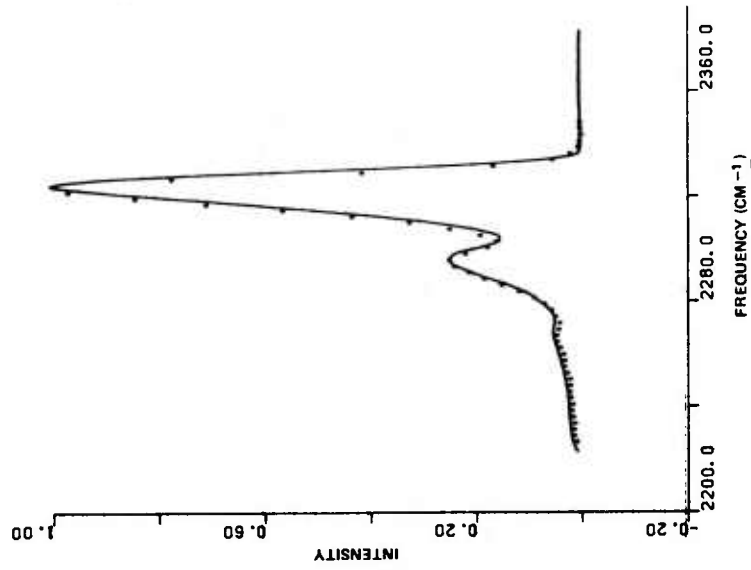


Figure 12. Experimental (•) and calculated N<sub>2</sub> CARS spectra for 0.81 equivalence ratio propane/air flame at T = 1,930 K (nonplanar CARS)

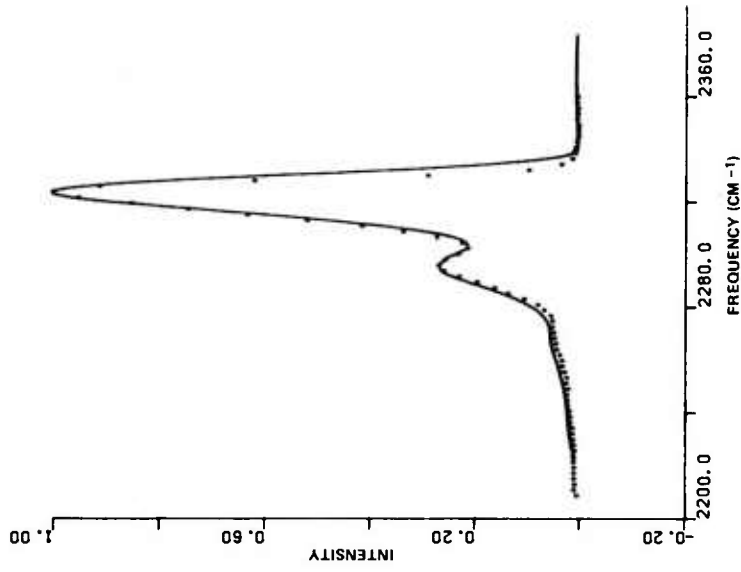


Figure 13. Experimental (•) and calculated N<sub>2</sub> CARS spectra for 1.02 equivalence ratio propane air flame at T = 2,020 K (planar CARS)

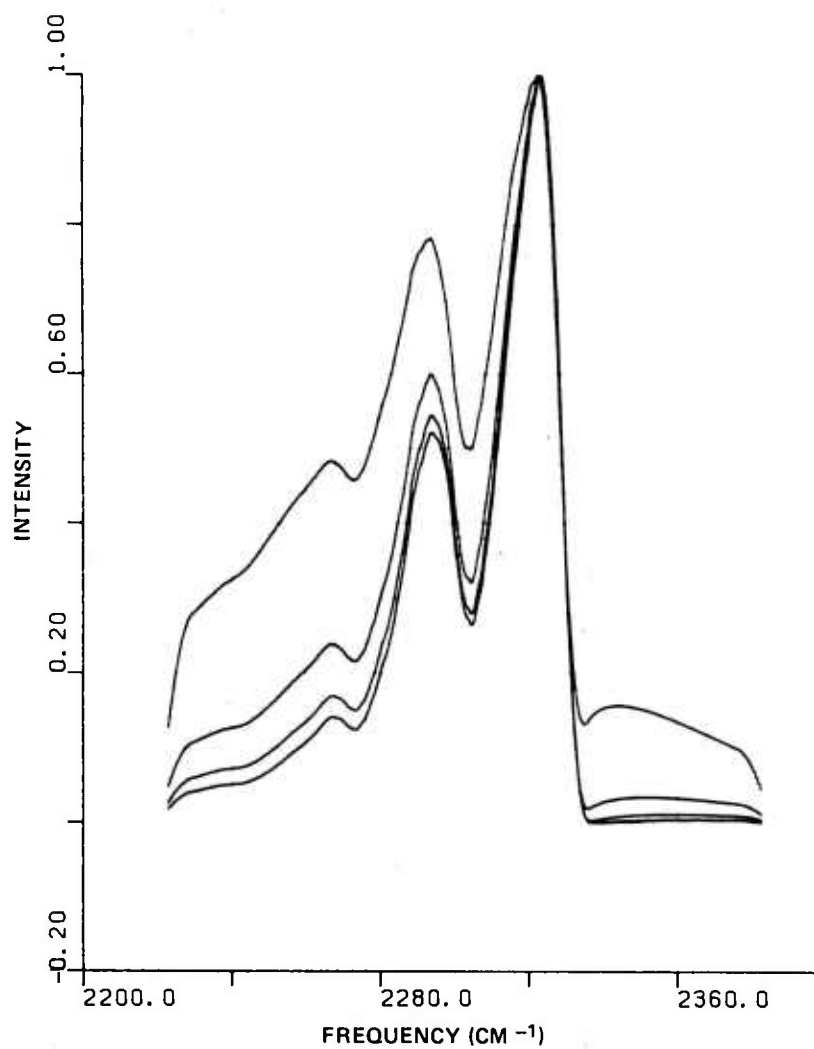


Figure 14. Calculated  $N_2$  CARS spectra at 2,500 K for flame products with 25, 50, 70, and 100% of the stoichiometric percentage of air

DISTRIBUTION LIST

Administrator  
Defense Technical Information Center  
ATTN: Accessions Division (12)  
Cameron Station  
Alexandria, VA 22314

Director  
Defense Advanced Research Projects Agency  
ATTN: LTC C. Buck  
1400 Wilson Boulevard  
Arlington, VA 22209

Director  
Institute for Defense Analyses  
ATTN: H. Wolfhard  
R. T. Oliver  
400 Army-Navy Drive  
Arlington, VA 22202

Commander  
U.S. Army Materiel Development  
and Readiness Command  
ATTN: DRCDMD-ST  
5001 Eisenhower Avenue  
Alexandria, VA 22333

Commander  
U.S. Army Armament Research  
and Development Command  
ATTN: DRDAR-TSS (5)  
DRDAR-GCL  
DRDAR-LC, J. Frasier  
DRDAR-LCA, A. Moss  
DRDAR-LCA-G, J. Lannon  
D. Downs  
L. Harris (10)  
T. Vladimiroff  
A. Beardell  
Y. Carignon  
DRDAR-LCE, R. Walker  
P. Marinkas  
C. Capellos  
F. Owens

Dover, NJ 07801

Commander  
U.S. Army Armament Materiel  
Readiness Command  
ATTN: DRSAR-LEP-L  
Rock Island, IL 61299

Chief  
Benet Weapons Laboratory, LCWSL  
U.S. Army Armament Research  
and Development Command  
ATTN: DRDAR-LCB-TL  
Watervliet, NY 12189

Commander  
U.S. Army Watervliet Arsenal  
ATTN: SARWV-RD, R. Thierry  
Watervliet, NY 12189

Commander  
U.S. Army Aviation Research  
and Development Command  
ATTN: DRSAV-E  
P.O. Box 209  
St. Louis, MO 63166

Director  
U.S. Army Air Mobility Research  
and Development Laboratory  
Ames Research Center  
Moffett Field, CA 94035

Commander  
U.S. Army Communications Research  
and Development Command  
ATTN: DRDCO-PPA-SA  
Fort Monmouth, NJ 07703

Commander  
U.S. Army Electronics Research  
and Development Command  
Technical Support Activity  
ATTN: DELSD-L  
Fort Monmouth, NJ 07703

Commander  
U.S. Army Missile Command  
ATTN: DRSMI-R  
DRSMI-YDL  
Redstone Arsenal, AL 35809

Commander  
U.S. Army Natick Research  
and Development Command  
ATTN: DRXRE, D. Sieling  
Natick, MA 01762

Commander  
U.S. Army Tank Automotive Research  
and Development Command  
ATTN: DRDTA-UL  
Warren, MI 48090

Commander  
U.S. Army White Sands Missile Range  
ATTN: STEWS-VT  
White Sands Missile Range, NM 88002

Commander  
U.S. Army Materials and  
Mechanics Research Center  
ATTN: DRXMR-ATL  
Watertown, MA 02172

Commander  
U.S. Army Research Office  
ATTN: Technical Library  
D. Squire  
F. Schmiedeshaff  
R. Ghirardelli  
M. Ciftan  
P.O. Box 12211  
Research Triangle Park, NC 27706

Director  
U.S. Army TRADOC Systems  
Analysis Activity  
ATTN: ATAA-SL  
White Sands Missile Range, NM 88002

Office of Naval Research  
ATTN: Code 473  
G. Neece  
800 N. Quincy Street  
Arlington, VA 22217

Commander  
Naval Sea Systems Command  
ATTN: J. W. Murrin, SEA-62R2  
National Center  
Bldg 2, Room 6E08  
Washington, DC 20362

Commander  
Naval Surface Weapons Center  
ATTN: Library Branch, DX-21  
Dahlgren, VA 22448

Commander  
Naval Surface Weapons Center  
ATTN: Code 240, S. J. Jacobs  
Code 730  
Silver Spring, MD 20910

Commander  
Naval Underwater Systems Center  
Energy Conversion Department  
ATTN: Code 5B331, R. S. Lazar  
Newport, RI 02840

Commander  
Naval Weapons Center  
ATTN: R. Derr  
C. Thelen  
China Lake, CA 93555

Commander  
Naval Research Laboratory  
ATTN: Code 6180  
Washington, DC 20375

Superintendent  
Naval Postgraduate School  
ATTN: Technical Library  
D. Netzer  
A. Fuhs  
Monterey, CA 93940

Commander  
Naval Ordnance Station  
ATTN: Dr. Charles Dale  
Technical Library  
Indian Head, MD 20640

AFOSR  
ATTN: J. F. Masi  
B. T. Wolfson  
D. Ball  
L. Caveny  
Bolling AFB, DC 20332

AFRPL (DYSC)  
ATTN: D. George  
J. N. Levine  
Edwards AFB, CA 93523

National Bureau of Standards  
ATTN: J. Hastie  
T. Kashiwagi  
Washington, DC 20234

Lockheed Palo Alto Research Laboratories  
ATTN: Technical Information Center  
3521 Hanover Street  
Palo Alto, CA 94304

Aerojet Solid Propulsion Co.  
ATTN: P. Micheli  
Sacramento, CA 95813

ARO Incorporated  
ATTN: N. Dougherty  
Arnold AFS, TN 37389

Atlantic Research Corporation  
ATTN: M. K. King  
5390 Cherokee Avenue  
Alexandria, VA 22314

AVCO Corporation  
AVCO Everett Research Laboratory Division  
ATTN: D. Stickler  
2385 Revere Beach Parkway  
Everett, MA 02149

Calspan Corporation  
ATTN: E. B. Fisher  
A. P. Trippe  
P.O. Box 400  
Buffalo, NY 14221

Foster Miller Associates, Inc.  
ATTN: A. J. Erickson  
135 Second Avenue  
Waltham, MA 02154

General Electric Company  
Armament Department  
ATTN: M. J. Bulman  
Lakeside Avenue  
Burlington, VT 05402

General Electric Company  
Flight Propulsion Division  
ATTN: Technical Library  
Cincinnati, OH 45215

Hercules Incorporated  
Alleghany Ballistic Lab  
ATTN: R. Miller  
Technical Library  
Cumberland, MD 21501

Hercules Incorporated  
Bacchus Works  
ATTN: B. Isom  
Magna, UT 84044

IITRI  
ATTN: M. J. Klein  
10 West 35th Street  
Chicago, IL 60615

Olin Corporation  
Badger Army Ammunition Plant  
ATTN: J. Ramnarace  
Baraboo, WI 53913

Olin Corporation  
New Haven Plant  
ATTN: R. L. Cook  
D. W. Riefler  
275 Winchester Avenue  
New Haven, CT 06504

Paul Gough Associates, Inc.  
ATTN: P. S. Gough  
P.O. Box 1614  
Portsmouth, NH 03801

Physics International Company  
2700 Merced Street  
Leandro, CA 94577

Pulsepower Systems, Inc.  
ATTN: L. C. Elmore  
815 American Street  
San Carlos, CA 94070

Rockwell International Corp.  
Rocketdyne Division  
ATTN: C. Obert  
    J. E. Flanagan  
    A. Axeworthy  
6633 Canoga Avenue  
Canoga Park, CA 91304

Rockwell International Corp.  
Rocketdyne Division  
ATTN: W. Haymes  
    Technical Library  
McGregor, TX 76657

Science Applications, Inc.  
ATTN: R. B. Edelman  
Combustion Dynamics and  
    Propulsion Division  
23146 Cumorah Crest  
Woodland Hills, CA 91364

Shock Hydrodynamics, Inc.  
ATTN: W. H. Anderson  
4710-16 Vineland Avenue  
N. Hollywood, CA 91602

Thiokol Corporation  
Elkton Division  
ATTN: E. Sutton  
Elkton, MD 21921

Thiokol Corporation  
Huntsville Division  
ATTN: D. Flanigan  
    R. Glick  
    Technical Library  
Huntsville, AL 35807

Thiokol Corporation  
Wasatch Division  
ATTN: J. Peterson  
    Technical Library  
P.O. Box 524  
Brigham City, UT 84302

TRW Systems Group  
ATTN: H. Korman  
One Space Park  
Redondo Beach, CA 90278

United Technologies  
Chemical Systems Division  
ATTN: R. Brown  
Technical Library  
P.O. Box 358  
Sunnyvale, CA 94086

Universal Propulsion Co.  
ATTN: H. J. McSpadden  
1800 W. Deer Valley road  
Phoenix, AZ 85027

Battelle Memorial Institute  
ATTN: Technical Library  
R. Bartlett  
505 King Avenue  
Columbus, OH 43201

Brigham Young University  
Department of Chemical Engineering  
ATTN: M. W. Beckstead  
Provo, UT 84601

California Institute of Technology  
204 Karmar Lab  
Mail Stop 301-46  
ATTN: F. E. C. Culick  
1201 E. California Street  
Pasadena, CA 91125

Case Western Reserve University  
Division of Aerospace Sciences  
ATTN: J. Tien  
Cleveland, OH 44135

Georgia Institute of Technology  
School of Aerospace Engineering  
ATTN: B. T. Zinn  
E. Price  
W. C. Strahle  
Atlanta, GA 30332

Institute of Gas Technology  
ATTN: D. Gidaspow  
3424 S. State Street  
Chicago, IL 60616

Johns Hopkins University/APL  
Chemical Propulsion Information Agency  
ATTN: T. Christian  
Johns Hopkins Road  
Laurel, MD 20810

Massachusetts Institute of Technology  
Department of Mechanical Engineering  
ATTN: T. Toong  
Cambridge, MA 02139

Pennsylvania State University  
Applied Research Laboratory  
ATTN: G. M. Faeth  
P.O. Box 30  
State College, PA 16801

Pennsylvania State University  
Department of Mechanical Engineering  
ATTN: K. Kuo  
Universtiy Park, PA 16801

Pennsylvania State University  
Department of Material Sciences  
ATTN: H. Palmer  
University Park, PA 16801

Princeton Combustion Research Laboratories  
ATTN: M. Summerfield  
1041 U.S. Highway One North  
Princeton, NJ 08540

Princeton University  
Forrestal Campus  
ATTN: I. Glassman  
Technical Library  
P.O. Box 710  
Princeton, NJ 08540

Purdue University  
School of Mechanical Engineering  
ATTN: J. Osborn  
S. N. B. Murthy  
TSPC Chaffee Hall  
W. Lafayette, IN 47906

Rutgers State University  
Department of Mechanical and  
Aerospace Engineering  
ATTN: S. Temkin  
University Heights Campus  
New Brunswick, NJ 08903

SRI International  
ATTN: Technical Library  
D. Crosley  
J. Barker  
D. Golden  
333 Ravenswood Avenue  
Menlo Park, CA 94025

Stevens Institute of Technology  
Davidson Library  
ATTN: R. McAlevy, III  
Hoboken, NJ 07030

United Technology  
ATTN: Alan Ecbreth  
Research Center  
East Hartford, CT 06108

Director  
U.S. Army Materiel Systems  
Analysis Activity  
ATTN: DRXSY-MP  
Aberdeen Proving Ground, MD 21005

Commander/Director  
Chemical Systems Laboratory  
U.S. Army Armament Research  
and Development Command  
ATTN: DRDAR-CLJ-L  
DRDAR-CLB-PA  
APG, Edgewood Area, MD 21010

Director  
Ballistics Research Laboratory  
U.S. Army Armament Research  
and Development Command  
ATTN: DRDAR-TSB-S  
DRDAR-BLP, L. Watermier  
A. Barrows  
C. Nelson  
J. Vanderhoff  
J. Anderson  
Aberdeen Proving Ground, MD 21005